

HALL EFFECTS ON UNSTEADY CONVECTIVE HEAT AND MASS TRANSFER FLOW IN A VERTICAL WAVY CHANNEL WITH TRAVELLING THERMAL WAVES

Sapna¹, Devika S^{2*} and Veena P H³

¹Research Scholar, Department of Mathematics, Gulbarga University, Gulbarga, Karnataka, India

²Guest Faculty Dept of Mathematics, Central University of Karnataka, Gulbarga, Karnataka, India

³Associate Professor, V G Women's College Gulbarga, Karnataka, India

(Received on: 29-04-13; Revised & Accepted on: 03-06-13)

ABSTRACT

Here the chemical reaction effect on mixed convective heat and mass transfer flow under the influence of an inclined magnetic field of a viscous, electrically conducting fluid through a porous medium in a vertical, electrically conducting fluid through a porous medium in a vertical wavy channel with heat sources is examined. The equations governing the flow, heat and mass transfer are solved by employing perturbation technique with aspect ratio δ is perturbation parameter. The velocity, temperature distributions are investigated for different values of governing parameters and the rate of heat and mass transfer are numerically evaluated.

Keywords: Unsteady convective flow, Hall Effect, Heat and mass transfer, Radiation Effect, chemical reaction, porous medium, travelling thermal waves and vertical wavy channel.

1. INTRODUCTION

Combined heat and Mass transfer problems with chemical reaction are of importance in many processes and have, therefore, received a considerable amount of attention in recent years. In processes such as drying, evaporation at the surface of a water body, energy transfer in a wet cooling tower and the flow in a desert cooler, heat and mass transfer occur simultaneously. Possible applications of this type of flow can be found in many industries. For example, in the power industry, among the methods of generating electric power is one in which electrical energy is extracted directly from a moving conducting fluid.

We are particularly interested in cases in which diffusion and chemical reaction occur at roughly the same speed. When diffusion is much faster than chemical reaction, then only chemical factors influence the chemical reaction rate; when diffusion is not much faster than reaction, the diffusion and kinetics interact to produce very different effects. The study of heat generation or absorption effects in moving fluids is important in view of several physical problems, such as fluids undergoing exothermic or endothermic chemical reaction. Due to the fast growth of electronic technology, effective cooling of electronic equipment has become warranted and cooling of electronic equipment ranges from individual transistors to main frame computers and from energy suppliers to telephone switch boards and thermal diffusion effect has been utilized for isotopes separation in the mixture between gases with very light molecular weight (hydrogen and helium) and medium molecular weight.

Muthucumaraswamy and Ganesan [5] studied effect of the chemical reaction and injection on flow characteristics in an insteady upward motion of an unsteady upward motion of an isothermal plate. Raptis and Perdakis [6] studied the unsteady free convection flow of water near C in the laminar boundary layer over a vertical moving porous plate.

The flows through a porous media under gravitational fields that are driven by gradients of fluid density caused by temperature gradient. Many studies, including most of the earlier work, have dealt with systems heated from below. Some attention has also been given to investigations of free convection in porous media introduced by a temperature gradient normal to the gravitational field. Raptis [7] has investigated unsteady free convective flow through a porous medium.

Corresponding author: Devika S^{2*}

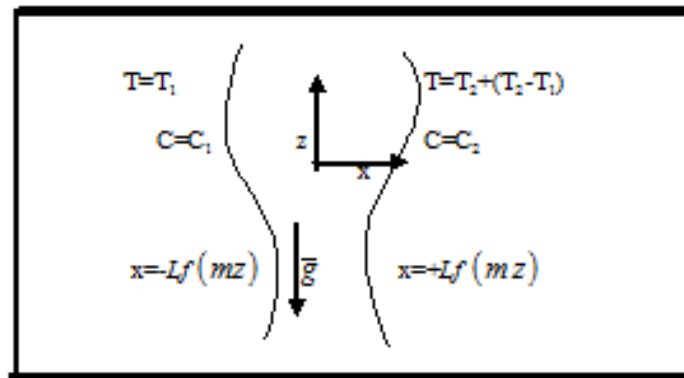
²Guest Faculty Dept of Mathematics, Central University of Karnataka, Gulbarga, Karnataka, India

Convection fluid flows generated by traveling thermal waves have also received attention due to applications in physical problems. The linearised analysis of these flows has shown that a traveling thermal wave can generate a mean shear flow within a layer of fluid, and the induced mean flow is proportional to the square of the amplitude of the wave. From a physical point of view, the motion induced by traveling thermal waves is quite interesting as a purely fluid-dynamical problem and can be used as a possible explanation for the observed four-day retrograde zonal motion of the upper atmosphere of Venus. Also, the heat transfer results will have a definite bearing on the design of oil-or gas –fired boilers.

Heat generation in a porous media due to the presence of temperature dependent heat sources has number of applications related to the development of energy resources. It is also important in engineering processes pertaining to flows in which a fluid supports an exothermic chemical or nuclear reaction. Proposal of disposing the radioactive waste material burying in the ground or in deep ocean sediment is another problem where heat generation in porous medium occurs. Radiative mixed convective mass transfer flow past an isothermal porous plate in the presence of thermal diffusion and heat generation was studied by Annupama *et al.*, [1]. The effect of chemical reaction on the unsteady convective heat and mass transfer flow of a viscous fluid in a vertical wavy channel with oscillatory flux and heat sources is recently examined by Devika *et al.*, [8]

In all these investigations, the effects of Hall currents are not considered. However, in a partially ionized gas, there occurs a Hall current when the strength of the impressed magnetic field is very strong. These Hall effects play a significant role in determining the flow features. Alam *et. al.*, [2] have studied unsteady free convective heat and mass transfer flow in a rotating system with Hall currents, viscous dissipation and Joule heating. Taking Hall effects in to account Krishan *et. al.*, [3, 4] have investigated Hall effects on the unsteady hydromagnetic boundary layer flow. Recently Seth *et. al.*, [10] have investigated the effects of Hall currents on heat transfer in a rotating MHD channel flow in arbitrary conducting walls. Sarkar *et. al.*, [9] have analyzed the effects of mass transfer and rotation and flow past a porous plate in a porous medium with variable suction in slip flow region.

In this paper we investigate the effect of chemical reaction on mixed convective heat and mass transfer flow of a viscous, electrically conducting fluid through a porous medium in a vertical wavy channel under the influence of an inclined magnetic field with heat sources. The equations governing the flow, heat and mass transfer are solved by employing perturbation technique with aspect ratio δ as perturbation parameter. The velocity, temperature and concentration distributions are investigated for different values of governing parameters. The rate of heat and mass transfer are numerically evaluated for different variations of the governing parameters.



Configuration of the Problem

2. FORMULATION AND SOLUTION OF THE PROBLEM

We consider the unsteady flow of an incompressible, viscous, electrically conducting fluid confined in a vertical channel bounded by two wavy walls under the influence of an inclined magnetic field of intensity H_0 lying in the plane (x-z). The magnetic field is inclined at an angle α_1 to the axial direction and hence its components are $(0, H_0 \sin(\alpha_1), H_0 \cos(\alpha_1))$. In view of the traveling thermal wave imposed on the wall $x = +Lf(mz)$ the velocity field has components $(u, 0, w)$. The magnetic field in the presence of fluid flow induces the current $(J_x, 0, J_z)$. We choose a rectangular Cartesian co-ordinate system $o(x, y, z)$ with z-axis in the vertical direction and the walls at $x = \pm Lf(mz)$.

When the strength of the magnetic field is very large we include the Hall current so that the generalized Ohm's law is modified to

$$\bar{J} + \omega_e \tau_e \bar{J} \times \bar{H} = \sigma (\bar{E} + \mu_e \bar{q} \times \bar{H}) \quad (1)$$

where \vec{q} is the velocity vector. \vec{H} is the magnetic field intensity vector. \vec{E} is the electric field, \vec{J} is the current density vector, ω_e is the cyclotron frequency, τ_e is the electron collision time, σ is the fluid conductivity and μ_e is the magnetic permeability. Neglecting the electron pressure gradient, ion-slip and thermo-electric effects and assuming the electric field $E=0$, equation (1) reduces

$$J_x - m H_0 J_z \sin(\alpha_1) = -\sigma \mu_e H_0 w \sin(\alpha_1) \quad (2)$$

$$J_z + m H_0 J_x \sin(\alpha_1) = \sigma \mu_e H_0 u \sin(\alpha_1) \quad (3)$$

where $m = \omega_e \tau_e$ is the Hall parameter.

On solving equations (2) & (3) we obtain

$$J_x = \frac{\sigma \mu_e H_0 \sin(\alpha_1)}{1 + m^2 H_0^2 \sin^2(\alpha_1)} (m H_0 \sin(\alpha_1) - w) \quad (4)$$

$$J_z = \frac{\sigma \mu_e H_0 \sin(\alpha_1)}{1 + m^2 H_0^2 \sin^2(\alpha_1)} (u + m H_0 w \sin(\alpha_1)) \quad (5)$$

where u , w are the velocity components along x and z directions respectively,

The Momentum equations are,

$$\frac{\partial u}{\partial t} + u \frac{\partial u}{\partial x} + w \frac{\partial u}{\partial z} = -\frac{\partial p}{\partial x} + \mu \left(\frac{\partial^2 u}{\partial x^2} + \frac{\partial^2 u}{\partial z^2} \right) + \mu_e (-H_0 J_z \sin(\alpha_1)) \quad (6)$$

$$\frac{\partial w}{\partial t} + u \frac{\partial w}{\partial x} + w \frac{\partial w}{\partial z} = -\frac{\partial p}{\partial z} + \mu \left(\frac{\partial^2 w}{\partial x^2} + \frac{\partial^2 w}{\partial z^2} \right) + \mu_e (H_0 J_x \sin(\alpha_1)) \quad (7)$$

Substituting J_x and J_z from equations (4) & (5) in equations (6) & (7) we obtain

$$\frac{\partial u}{\partial t} + u \frac{\partial u}{\partial x} + w \frac{\partial u}{\partial z} = -\frac{\partial p}{\partial x} + \mu \left(\frac{\partial^2 u}{\partial x^2} + \frac{\partial^2 u}{\partial z^2} \right) - \frac{\sigma \mu_e H_0^2 \sin^2(\alpha_1)}{1 + m^2 H_0^2 \sin^2(\alpha_1)} (u + m H_0 w \sin(\alpha_1)) - \rho g \quad (8)$$

$$\frac{\partial w}{\partial t} + u \frac{\partial w}{\partial x} + w \frac{\partial w}{\partial z} = -\frac{\partial p}{\partial z} + \mu \left(\frac{\partial^2 w}{\partial x^2} + \frac{\partial^2 w}{\partial z^2} \right) - \frac{\sigma \mu_e H_0^2 \sin^2(\alpha_1)}{1 + m^2 H_0^2 \sin^2(\alpha_1)} (w - m H_0 u \sin(\alpha_1)) \quad (9)$$

The energy equation is

$$\rho C_p \left(\frac{\partial T}{\partial t} + u \frac{\partial T}{\partial x} + w \frac{\partial T}{\partial z} \right) = k_f \left(\frac{\partial^2 T}{\partial x^2} + \frac{\partial^2 T}{\partial z^2} \right) + Q(T_0 - T) \quad (10)$$

The diffusion equation is

$$\left(\frac{\partial C}{\partial t} + u \frac{\partial C}{\partial x} + w \frac{\partial C}{\partial z} \right) = D_{1f} \left(\frac{\partial^2 C}{\partial x^2} + \frac{\partial^2 C}{\partial z^2} \right) - k_1 (C - C_0) \quad (11)$$

The equation of state is

$$\rho - \rho_0 = -\beta(T - T_0) - \beta^*(C - C_0) \quad (12)$$

where T, C are the temperature and concentration in the fluid. k_f is the thermal conductivity, C_p is the specific heat constant pressure, β is the coefficient of thermal expansion, β^* is the volumetric coefficient of expansion with mass fraction coefficient, D_1 is the molecular diffusivity, Q is the strength of the heat source, k_{11} is the cross diffusivity, k_1 is the chemical reaction coefficient.

The flow is maintained by a constant volume flux for which a characteristic velocity is defined as

$$q = \frac{1}{L} \int_{-L_f}^{L_f} w dz \quad (13)$$

The boundary conditions are

$$u=0, w=0, T=T_1, C=C_1 \text{ on } x = -L_f(mz) \quad (14)$$

$$w=0, w=0, T=T_2 + ((T_1-T_2) \sin(mz+nt)), C=C_2 \text{ on } x = -L_f(mz) \quad (15)$$

Eliminating the pressure from equations (8) & (9) and introducing the Stokes Stream function ψ as

$$u = -\frac{\partial \psi}{\partial z}, w = \frac{\partial \psi}{\partial x} \quad (16)$$

the equations (8), (9), (11) in terms of ψ are

$$\frac{\partial(\nabla^2 \psi)}{\partial t} - \frac{\partial \psi}{\partial z} \frac{\partial(\nabla^2 \psi)}{\partial x} + \frac{\partial \psi}{\partial x} \frac{\partial(\nabla^2 \psi)}{\partial z} = \mu \nabla^4 \psi + \beta g \frac{\partial(T-T_e)}{\partial x} + \beta^* g \frac{\partial(C-C_e)}{\partial x} - \left(\frac{\sigma \mu_e^2 H_0^2 \sin^2(\alpha_1)}{1+m^2 H_0^2 \sin^2(\alpha_1)} \right) \nabla^2 \psi \quad (17)$$

$$\rho C_p \left(\frac{\partial T}{\partial t} + \frac{\partial \psi}{\partial x} \frac{\partial T}{\partial z} - \frac{\partial \psi}{\partial z} \frac{\partial T}{\partial x} \right) = k_f \left(\frac{\partial^2 T}{\partial x^2} + \frac{\partial^2 T}{\partial z^2} \right) + Q(T-T_e) \quad (18)$$

$$\left(\frac{\partial C}{\partial t} + \frac{\partial \psi}{\partial x} \frac{\partial C}{\partial z} - \frac{\partial \psi}{\partial z} \frac{\partial C}{\partial x} \right) = D_1 \left(\frac{\partial^2 C}{\partial x^2} + \frac{\partial^2 C}{\partial z^2} \right) - k_1(C-C_0) \quad (19)$$

On introducing the following non-dimensional variables

$$(x', z') = (x, mz/L), \psi' = \frac{\psi}{qL}, \theta = \frac{T-T_2}{T_1-T_2}, C' = \frac{C-C_2}{C_1-C_2}$$

the equation of momentum and energy in the non-dimensional form are

$$\nabla^4 \psi - M_1^2 \nabla^2 \psi + \frac{G}{R} \left(\frac{\partial \theta}{\partial z} + N \frac{\partial C}{\partial z} \right) = \delta R \left(\delta \frac{\partial}{\partial t} (\nabla^2 \psi) + \left(\frac{\partial \psi}{\partial z} \frac{\partial(\nabla^2 \psi)}{\partial x} - \frac{\partial \psi}{\partial x} \frac{\partial(\nabla^2 \psi)}{\partial z} \right) \right) \quad (20)$$

$$\delta P \left(\delta \frac{\partial \theta}{\partial t} + \frac{\partial \psi}{\partial x} \frac{\partial \theta}{\partial z} - \frac{\partial \psi}{\partial z} \frac{\partial \theta}{\partial x} \right) = \left(\frac{\partial^2 \theta}{\partial x^2} + \delta^2 \frac{\partial^2 \theta}{\partial z^2} \right) - \alpha \theta \quad (21)$$

$$\delta Sc \left(\delta \frac{\partial C}{\partial t} + \frac{\partial \psi}{\partial x} \frac{\partial C}{\partial z} - \frac{\partial \psi}{\partial z} \frac{\partial C}{\partial x} \right) = \left(\frac{\partial^2 C}{\partial x^2} + \delta^2 \frac{\partial^2 C}{\partial z^2} \right) - KC \quad (22)$$

$$\nabla^2 = \frac{\partial}{\partial x^2} + \delta^2 \frac{\partial}{\partial z^2}$$

$$\begin{array}{ll}
 \text{where } G = \frac{\beta g \Delta T_e L^3}{\nu^2} & \text{(Grashof Number)} \\
 M^2 = \frac{\sigma \mu_e^2 H_o^2 L^2}{\nu^2} & \text{(Hartman Number)} \\
 R = \frac{qL}{\nu} & \text{(Reynolds Number)} \\
 \alpha = \frac{QL^2}{K_f(T_1 - T_2)} & \text{(Heat Source Parameter)} \\
 N = \frac{\beta^*(C_1 - C_2)}{\beta(T_1 - T_2)} & \text{(Buoyancy ratio)} \\
 \delta = mL & \text{(Aspect ratio)} \\
 M_1^2 = \frac{M^2 \sin^2(\alpha_1)}{1 + m^2} \\
 P = \frac{\mu C_p}{K_f} & \text{(Prandtl Number)} \\
 Sc = \frac{\nu}{D_1} & \text{(Schmidt Number)} \\
 k = \frac{k_1 L^2}{D_1} & \text{(Chemical reaction parameter)}
 \end{array}$$

The corresponding boundary conditions are

$$\psi(1) - \psi(-1) = 1$$

$$\frac{\partial \psi}{\partial z} = 0, \frac{\partial \psi}{\partial x} = 0, \theta = 1, C = 1 \quad \text{at } x = -f(z)$$

$$\frac{\partial \psi}{\partial z} = 0, \frac{\partial \psi}{\partial x} = 0, \theta = \sin(z + \gamma t), C = 0 \quad \text{at } x = +f(z) \quad (23)$$

3. ANALYSIS OF THE FLOW

On introducing the transformation

$$\eta = \frac{x}{f(z)} \quad (24)$$

The equations (20)-(22) reduce to

$$F^4 \psi - (M_1^2 f^2) F^2 \psi + \left(\frac{Gf^3}{R} \right) \left(\frac{\partial \theta}{\partial z} + N \frac{\partial C}{\partial z} \right) = (\delta R f) \left(\delta \frac{\partial}{\partial t} (F^2 \psi) \right) + \left(\frac{\partial \psi}{\partial z} \frac{\partial (F^2 \psi)}{\partial \eta} - \frac{\partial \psi}{\partial \eta} \frac{\partial (F^2 \psi)}{\partial z} \right) \quad (25)$$

$$(\delta P f) \left(\delta \frac{\partial \theta}{\partial t} + \frac{\partial \psi}{\partial \eta} \frac{\partial \theta}{\partial z} - \frac{\partial \psi}{\partial z} \frac{\partial \theta}{\partial \eta} \right) = \left(\frac{\partial^2 \theta}{\partial \eta^2} + \delta^2 f^2 \frac{\partial^2 \theta}{\partial z^2} \right) - (\alpha f^2) \theta \quad (26)$$

$$(\delta S c f) \left(\delta f^2 \frac{\partial C}{\partial t} + \frac{\partial \psi}{\partial \eta} \frac{\partial C}{\partial z} - \frac{\partial \psi}{\partial z} \frac{\partial C}{\partial \eta} \right) = \left(\frac{\partial^2 C}{\partial \eta^2} + \delta^2 f^2 \frac{\partial^2 C}{\partial z^2} \right) - (K f^2) C \quad (27)$$

Assuming the aspect ratio δ to be small we take the asymptotic solutions as

$$\left. \begin{array}{l}
 \psi(x, z, t) = \psi_0(x, z, t) + \delta \psi_1(x, z, t) + \delta^2 \psi_2(x, z, t) + \dots \\
 \theta(x, z, t) = \theta_0(x, z, t) + \delta \theta_1(x, z, t) + \delta^2 \theta_2(x, z, t) + \dots \\
 C(x, z, t) = C_0(x, z, t) + \delta C_1(x, z, t) + \delta^2 C_2(x, z, t) + \dots
 \end{array} \right\} \quad (28)$$

Substituting (28) in equations (25)-(27) and equating the like powers of δ the equations and the respective boundary conditions to the zeroth order are

$$\frac{\partial^2 \theta_0}{\partial \eta^2} - (\alpha f^2) \theta_0 = 0 \quad (29)$$

$$\frac{\partial^2 C_0}{\partial \eta^2} - (kf^2)C_0 = 0 \quad (30)$$

$$\frac{\partial^4 \psi_0}{\partial \eta^4} - (M_1^2 f^2) \frac{\partial^2 \psi_0}{\partial \eta^2} = - \left(\frac{Gf^3}{R} \right) \left(\frac{\partial \theta_0}{\partial z} + N \frac{\partial C_0}{\partial z} \right) \quad (31)$$

with

$$\left. \begin{aligned} \psi_0(+1) - \psi_0(-1) &= 1 \\ \frac{\partial \psi_0}{\partial \eta} &= 0, \quad \frac{\partial \psi_0}{\partial \bar{z}} = 0, \quad \theta_0 = 1, \quad C_0 = 1 \quad \text{at } \eta = -1 \\ \frac{\partial \psi_0}{\partial \eta} &= 0, \quad \frac{\partial \psi_0}{\partial \bar{z}} = 0, \quad \theta_0 = \sin(z + \gamma t), \quad C_0 = 0 \quad \text{at } \eta = +1 \end{aligned} \right\} \quad (32)$$

and to the first order are

$$\frac{\partial^2 \theta_1}{\partial \eta^2} - (\alpha f^2) \theta_1 = (PRf) \left(\frac{\partial \psi_0}{\partial \eta} \frac{\partial \theta_0}{\partial \bar{z}} - \frac{\partial \psi_0}{\partial \bar{z}} \frac{\partial \theta_0}{\partial \eta} \right) \quad (33)$$

$$\frac{\partial^2 C_1}{\partial \eta^2} - (kf^2)C_1 = (ScRf) \left(\frac{\partial \psi_0}{\partial \mu} \frac{\partial C_0}{\partial \bar{z}} - \frac{\partial \psi_0}{\partial \bar{z}} \frac{\partial C_0}{\partial \eta} \right) \quad (34)$$

$$\frac{\partial^4 \psi_1}{\partial \eta^4} - (M_1^2 f^2) \frac{\partial^2 \psi_1}{\partial \eta^2} = - \left(\frac{Gf^3}{R} \right) \left(\frac{\partial \theta_1}{\partial z} + N \frac{\partial C_1}{\partial z} \right) + (Rf) \left(\frac{\partial \psi_0}{\partial \eta} \frac{\partial^3 \psi_0}{\partial z^3} - \frac{\partial \psi_0}{\partial \bar{z}} \frac{\partial^3 \psi_0}{\partial \eta \partial z^2} \right) \quad (35)$$

with

$$\left. \begin{aligned} \psi_1(+1) - \psi_1(-1) &= 0 \\ \frac{\partial \psi_1}{\partial \eta} &= 0, \quad \frac{\partial \psi_1}{\partial \bar{z}} = 0, \quad \theta_1 = 0, \quad C_1 = 0 \quad \text{at } \eta = -1 \\ \frac{\partial \psi_1}{\partial \eta} &= 0, \quad \frac{\partial \psi_1}{\partial \bar{z}} = 0, \quad \theta_1 = 0, \quad C_1 = 0 \quad \text{at } \eta = +1 \end{aligned} \right\} \quad (36)$$

4. SOLUTIONS OF THE PROBLEM

$$\theta_0 = 0.5\alpha(x^2 - 1) + 0.5\sin(z + \gamma t)(1 + x) + 0.5(1 - x)$$

$$C_0 = 0.5 \left(\frac{Ch(\beta_1 x)}{Ch(\beta_1)} - \frac{sh(\beta_1 x)}{sh(\beta_1)} \right) + a_3 \left(\frac{Ch(\beta_1 x)}{Ch(\beta_1)} - 1 \right)$$

$$\psi_0 = a_9 \cosh(M_1 x) + a_{10} \sinh(M_1 x) + a_{11} x + a_{12} + \phi_1(x) \quad \phi_1(x) = -a_6 x + a_7 x^2 - a_8 x^3$$

$$\begin{aligned} \theta_1 &= a_{36}(x^2 - 1) + a_{37}(x^3 - x) + a_{38}(x^4 - 1) + a_{39}(x^5 - x) + a_{40}(x^6 - 1) \\ &\quad + (a_{41} + xa_{43})(Ch(M_1 x) - Ch(M_1)) + a_{42}(Sh(M_1 x) - xSh(M_1)) \\ &\quad + a_{44}(xSh(M_1 x) - Sh(M_1)) \end{aligned}$$

$$\begin{aligned}
 C_1 = & a_{47} \left(1 - \frac{Ch(\beta_1 x)}{Ch(\beta_1)} \right) + a_{48} \left(x - \frac{S(\beta_1 x)}{Sh(\beta_1)} \right) + a_{49} \left(x^2 - \frac{Ch(\beta_1 x)}{Ch(\beta_1)} \right) \\
 & + a_{50} \left(x^3 - \frac{S(\beta_1 x)}{Sh(\beta_1)} \right) + a_{51} \left(x^4 - \frac{Ch(\beta_1 x)}{Ch(\beta_1)} \right) + a_{52} \left(Ch(M_1 x) - Ch(M_1) \frac{Ch(\beta_1 x)}{Ch(\beta_1)} \right) \\
 & + a_{53} \left(Sh(M_1 x) - Sh(M_1) \frac{Sh(\beta_1 x)}{Sh(\beta_1)} \right) + a_{54} \left(x Ch(M_1 x) - Ch(M_1) \frac{Sh(\beta_1 x)}{Sh(\beta_1)} \right) \\
 & + a_{55} \left(x Sh(M_1 x) - Sh(M_1) \frac{Ch(\beta_1 x)}{Ch(\beta_1)} \right) + b_3 \left(Sh(\beta_2 x) - Sh(\beta_2) \frac{Sh(\beta_1 x)}{Sh(\beta_1)} \right) \\
 & + b_4 \left(Sh(\beta_3 x) - Sh(\beta_3) \frac{S(\beta_1 x)}{Sh(\beta_1)} \right) + b_5 \left(Ch(\beta_2 x) - Ch(\beta_2) \frac{Ch(\beta_1 x)}{Ch(\beta_1)} \right) \\
 & + b_6 \left(Ch(\beta_3 x) - Ch(\beta_2) \frac{Ch(\beta_1 x)}{Ch(\beta_1)} \right) + b_7 \left(x Sh(\beta_1 x) - Sh(\beta_1) \frac{Ch(\beta_1 x)}{Ch(\beta_1)} \right) \\
 & + b_8 \left(x^2 Sh(\beta_1 x) - Sh(\beta_1) \frac{Ch(\beta_1 x)}{Ch(\beta_1)} \right) + b_9 \left(x^3 Sh(\beta_1 x) - Sh(\beta_1) \frac{Ch(\beta_1 x)}{Ch(\beta_1)} \right) \\
 & + b_{11} \left(x Ch(\beta_1 x) - Ch(\beta_1) \frac{Sh(\beta_1 x)}{Sh(\beta_1)} \right) + b_{12} (x^2 Ch(\beta_1 x) - Ch(\beta_1)) \\
 & + b_{13} \left(x^3 Ch(\beta_1 x) - Ch(\beta_1) \frac{Sh(\beta_1 x)}{Sh(\beta_1)} \right)
 \end{aligned}$$

$$\psi_1 = d_2 \cosh(M_1 x) + d_3 \sinh(M_1 x) + d_4 x + d_5 + \phi_4(x)$$

$$\begin{aligned}
 \phi_4(x) = & b_{65}x + b_{66}x^2 + b_{67}x^3 + b_{68}x^4 + b_{69}x^5 + b_{70}x^6 + b_{71}x^7 + (b_{72}x + \\
 & + b_{74}x^2 + b_{77}x^3) \cosh(M_1 x) + (b_{73}x + b_{75}x^2 + b_{76}x^3) \sinh(M_1 x) \\
 & + b_{78} \cosh(\beta_1 x) + b_{79} \sinh(\beta_1 x)
 \end{aligned}$$

5. NUSSELT NUMBER and SHERWOOD NUMBER

The rate of heat transfer (Nusselt Number) on the walls has been calculated using the formula

$$\begin{aligned}
 Nu = & \frac{1}{(\theta_m - \theta_w)} \left(\frac{\partial \theta}{\partial x} \right)_{x=\pm 1} \text{ where } \theta_m = 0.5 \int_{-1}^1 \theta dx, (Nu)_{x=+1} = \frac{1}{\theta_m - \sin(z + \gamma t)} (b_{24} + \delta b_{22}) \\
 (Nu)_{x=-1} = & \frac{1}{(\theta_m - 1)} (b_{25} + \delta b_{23}), \theta_m = b_{26} + \delta b_{27}
 \end{aligned}$$

The rate of mass transfer (Sherwood Number) on the walls has been calculated using the formula

$$\begin{aligned}
 Sh = & \frac{1}{(C_m - C_w)} \left(\frac{\partial C}{\partial x} \right)_{x=\pm 1} \text{ where } C_m = 0.5 \int_{-1}^1 C dx \quad (Sh)_{x=+1} = \frac{1}{C_m} (b_{18} + \delta b_{16}) \\
 (Sh)_{x=-1} = & \frac{1}{(C_m - 1)} (b_{19} + \delta b_{17}), \quad C_m = b_{20} + \delta b_{21} \quad \text{where } a_1, a_2, \dots, a_{90}, b_1, b_2, \dots, b_{79} \text{ are constants given in the} \\
 & \text{appendix}
 \end{aligned}$$

6. RESULTS AND DISCUSSION OF THE NUMERICAL RESULTS

In this analysis we investigate the effect of Hall Currents and radiation on mixed convective heat and mass transfer flow of a viscous, electrically conducting fluid in a vertical wavy channel with traveling thermal wave imposed on the wall in the presence of heat generating source under an inclined magnetic field.

1. Fig1 represents W with graph of number G . It is found that W exhibits a reversal flow for $G < 0$ and the reflow of reversal flow enlarges with increase in $G < 0$. The magnitude of W experiences an enhancement with $|G|$ with maximum increase occurring at $\eta = 0$. The variation of W with M and m shows that higher the Lorentz force smaller $|W|$ in the flow region. An increase in the Hall parameter m leads to an enhancement in W (fig.2). The variation of W with heat source parameter α shows that higher the strength of the heat source larger the axial velocity in the entire flow region (fig.3). The effect of surface geometry (β) on W is shown in fig.4. It is found that higher the dilation of the channel walls larger W in the flow region. Fig.5 represents W with chemical reaction parameter K . It is found that W exhibits a reversal flow for $k = 3.5$ and $|W|$ enhances with increase in K .
2. The secondary velocity (u) which arises due to the waviness of the boundary. Fig.6 represents u with G . It is found that the secondary velocity is towards the boundary for $G > 0$ and is towards the mid region for $G < 0$ $|u|$ enhances with increase in $|G|$. With maximum attained at $\eta = -0.4$. The variation of u with M and m shows that higher the Lorentz force smaller $|u|$ in the flow region. An increase in the hall parameter m leads to a depreciation u (fig.7). From figs. 8 & 9 we find that $|u|$ enhances with increase in α and β . Thus higher the dilation of the channel walls larger $|u|$ in the flow region. When the molecular buoyancy force dominates over the thermal buoyancy force $|u|$ depreciates irrespective of the directions of the buoyancy forces.
3. The non-dimensional temperature(θ) is shown for different variations of G , M , m , α , β and k Fig.10 represents the temperature with Grashof number G . We follow the convention that the non-dimensional temperature is positive or negative according as the actual temperature is greater /lesser than the equilibrium temperature. It is found that the actual temperature enhances with increase in $G > 0$ and reduces with $G < 0$. The variation of θ with M shows that higher the Lorentz force smaller the actual temperature in the left half and larger in the right half of the channel(fig.11).An increase in the Hall parameter $m \leq 1.5$ leads to an enhancement in the actual temperature in the left half and reduces in the right half while for higher $m \geq 2.5$ it depreciates in the entire flow region(fig.12). An increase in the heat source parameter α leads to an enhancement in the actual temperature in the entire flow region(fig.14).The influence of surface geometry on θ is shown in fig.15.It is observed that higher the dilation of the channel walls larger the actual temperature and for higher dilation we notice a depreciation in the left half and an enhancement in the right half of the channel. With respect to the chemical reaction parameter $k \leq 1.5$ we find that the actual temperature reduces in the left half and enhances in the right half and for higher $k \geq 2.5$ we find a depreciation in the entire flow region (fig.13).
4. The concentration distribution(C) is shown for different variations of the parameters.Fig.16 represents C with G . It is found that the actual concentration enhances with $G > 0$ and for $G < 0$, it enhances in the left half and reduces in the right half of the channel. Higher the Lorentz force smaller C in the left half and larger in the right half and for higher Lorentz force larger in the left half and smaller in the right half of the channel(18).An increase in the Hall parameter m reduces the concentration in the left half and enhances in the right half(fig.17). An increase in the chemical reaction parameter k results in a depreciation in the actual concentration in the entire flow region (fig.19). With respect to α we notice a depreciation in C in the left half and enhances in the right half(fig.21). The variation of C with β shows that higher the dilation of the channel walls smaller the actual concentration in the left half and larger in the right half (fig.22).

The rate of heat transfer(Nusselt Number) at $\eta = \pm 1$ is shown in tables.1-2 for different variations of k , α , R , β .It is found that the rate of heat transfer at $\eta = +1$ enhances with $G > 0$ and reduces with $G < 0$ while at $\eta = -1$, $|Nu|$ reduces with $G > 0$ and enhances with $G < 0$. $|Nu|$ enhances with increase in the strength of the heat source. With reference to the chemical reaction parameter k we find an enhancement in, $|Nu|$ with increase in $k \leq 1.5$ and depreciates with higher $k \geq 2.5$ at both the walls. Higher the dilation of the channel walls larger.

The rate of mass transfer (Sherwood Number) at the boundaries $\eta = \pm 1$ is shown in tables.3-4 for different variations of the governing parameters. It is found that the rate of mass transfer at $\eta = +1$ reduces with $G > 0$ and enhances with $G < 0$. At $\eta = -1$, $|Sh|$ reduces with $|G|$. With respect to α we find that the rate of mass transfer at $\eta = 1$, reduces with $\alpha \leq 4$ and for higher $\alpha \geq 6$, $|Sh|$ enhances in the heating case and reduces in the cooling case. At $\eta = -1$, $|Sh|$ reduces in the heating case and enhances in the cooling case with $\alpha \leq 4$ and for higher $\alpha \geq 6$. we notice an enhancement in $|Sh|$ for all G . Higher the dilation of the channel walls larger $|Sh|$ at both the walls. With respect to chemical reaction parameter k we find that, $|Sh|$ reduces at both the walls with increase in $k \leq 1.5$ and for higher $k \geq 2.5$.

7. REFERENCES

- [1] Anupama A, Venkata Ramana Reddy G., Jayarami Reddy K: Radiative mixed convective mass transfer flow past an isothermal porous plate in the presence of thermal diffusion and heat generation vol. 4 (3) 2013, pp 37- 46.
- [2] Alam M M and Sattar M A: Unsteady free convection and mass transfer flow in a rotating system with Hall currents, viscous dissipation and Joule heating, Journal of Energy heat and mass transfer, V.22, (2000) pp.31-39.
- [3] Krishna D V and Prasada rao D R V: Hall effects on the unsteady hydromagnetic boundary layer flow., Acta Mechanica,V.30, (1981) pp.303-309.
- [4] Krishna D V, Prasada rao D R V, Ramachandra Murty, A S: Hydromagnetic convection flow through a porous medium in a rotating channel., J.Engg. Phy. and Thermo.Phy,V.75(2), (2002) pp.281-291.
- [5] Muthucumaraswamy R, Ganesan P. Effect of the chemical reaction and injection on flow characteristics in an unsteady upward motion of an isothermal plate, J.Appl.Mech Tech Phys, 42, (2001) pp.665-671.
- [6] Raptis A, Perdikis C: Free convection flow of water near 4 C past a moving plate. Forschung Im Ingenieurwesen; Vol. 67: (2002) pp.206-208.
- [7] Raptis, A: Int. J. Engng.Sci, V.21, (1983) pp.345.
- [8] Sapna, Devika S, Veena P H: Effect of Chemical reaction on the unsteady convective heat and mass transfer flow of viscous fluid in a vertical wavy channel with oscillatory flux and heat sources vol 4 (3) 2013, pp1-9.
- [9] Sarkar D and Mukherjee S: Acta Ciencia Indica., V.34M, No.2, (2008), pp.737-751.
- [10] Seth, G.S, Ansari, S and Ahmad, N : Acta Ciencia Indica , V.34M, No.4, (2008) p.1849.

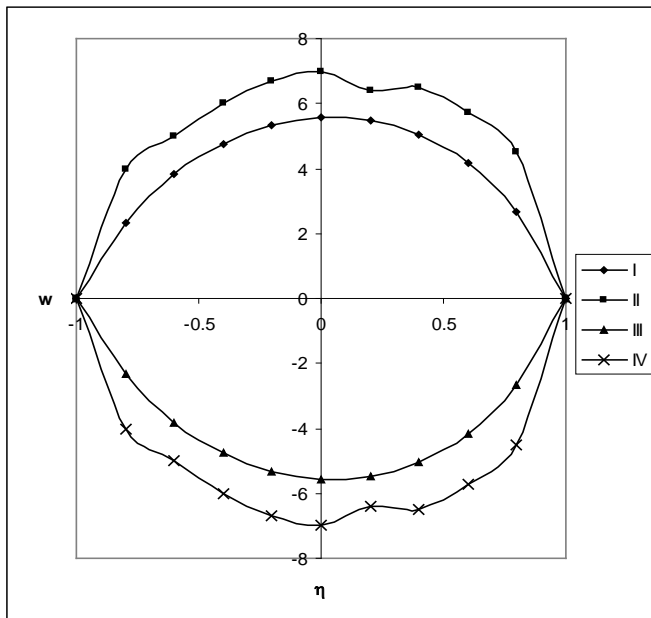


Fig.1: Variation of axial velocity (W) with G
M=2, m=0.5, Sc=1.3, $\alpha=2$, $\beta=0.5$, k=0.5

	I	II	III	IV
G	10^3	3×10^3	-10^3	-3×10^3

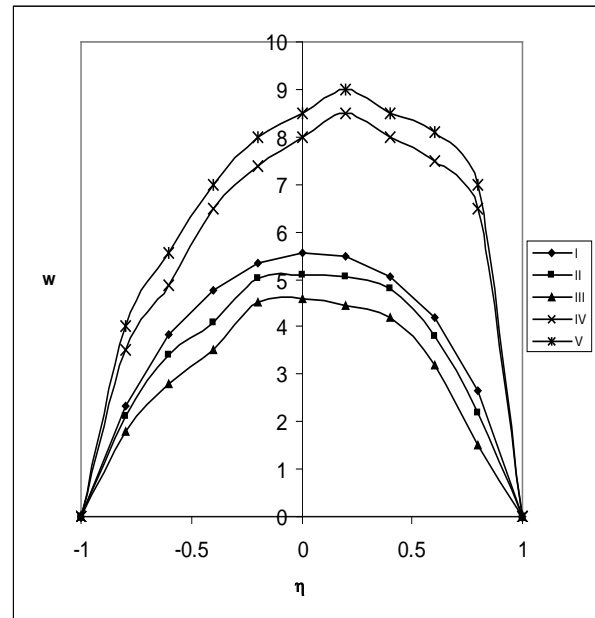


Fig.2: W with M & m

G= 10^3 , Sc=1.3, $\alpha=2$, $\beta=0.5$, k=0.5

	I	II	III	IV	V
M	2	5	10	2	2
m	0.5	0.5	0.5	1.5	2.5

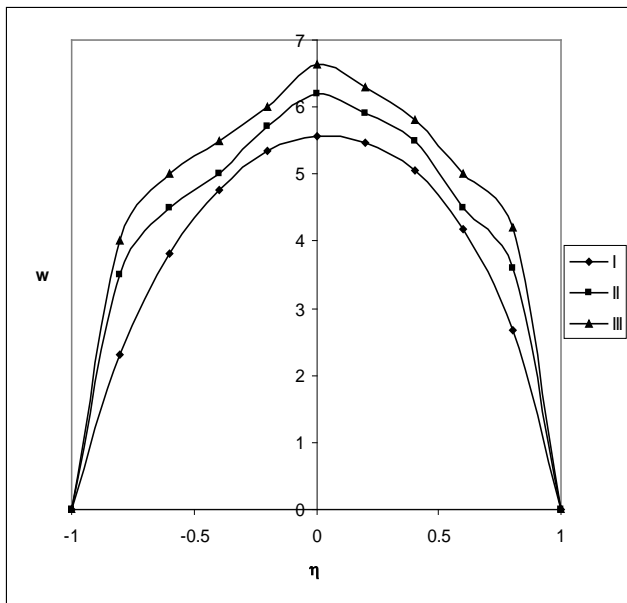


Fig.3: W with α
 $M=2, m=0.5, Sc=1.3, k=0.5, \beta$

	I	II	III
α	2	4	6

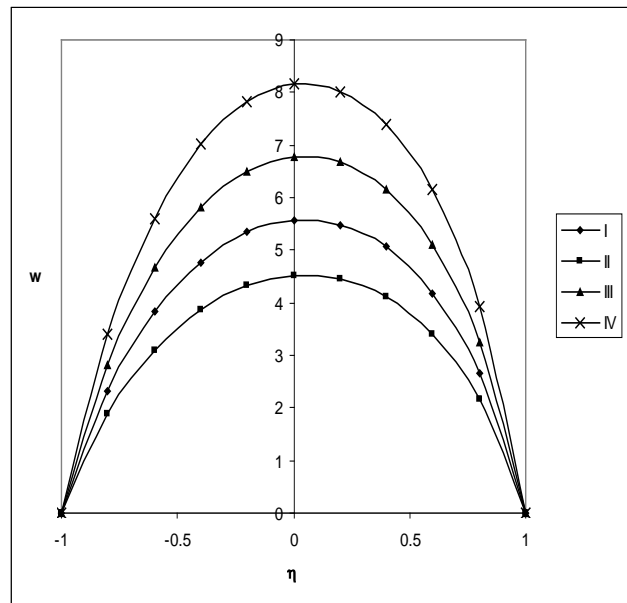


Fig.4: W with β
 $G=10^3, Sc=1.3, \alpha=2, k=0.5$

	I	II	III	IV
β	0.3	0.5	0.7	0.9

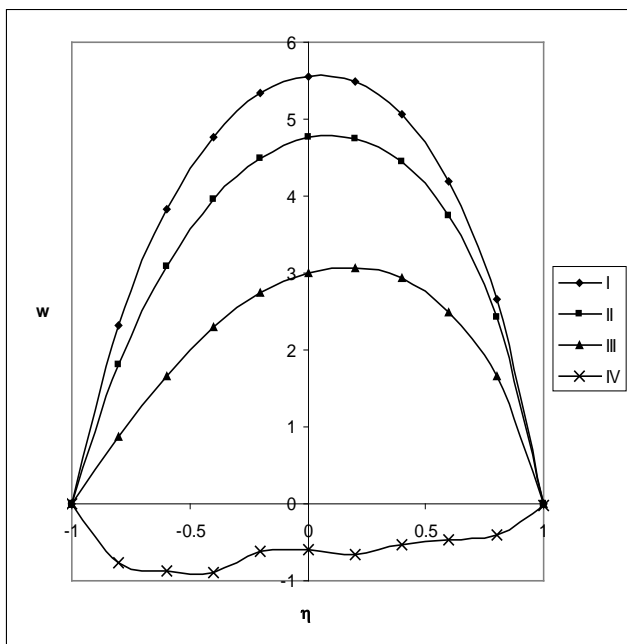


Fig.5: W with k
 $G=10^3, Sc=1.3, \alpha=2, \beta=0.5$

	I	II	III	IV
k	0.5	1.5	2.5	3.5

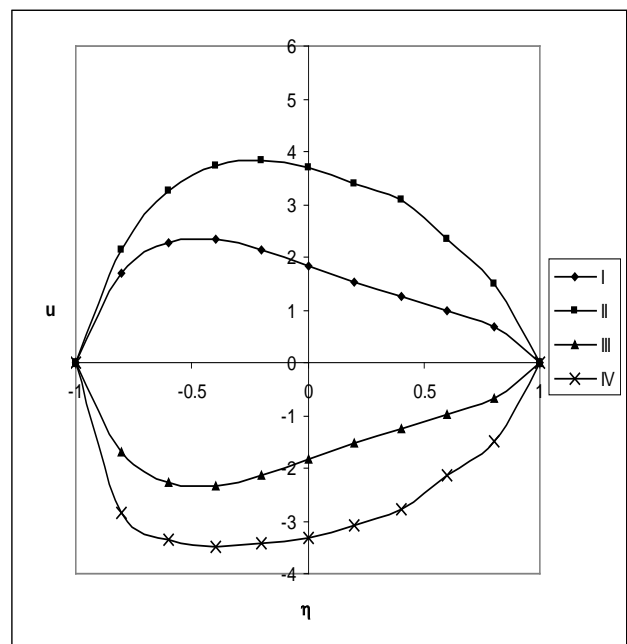


Fig.6: Variation of axial velocity (u) with G
 $M=2, m=0.5, Sc=1.3, \alpha=2, \beta=0.5, k=0.5$

	I	II	III	IV
G	10^3	3×10^3	-10^3	-3×10^3

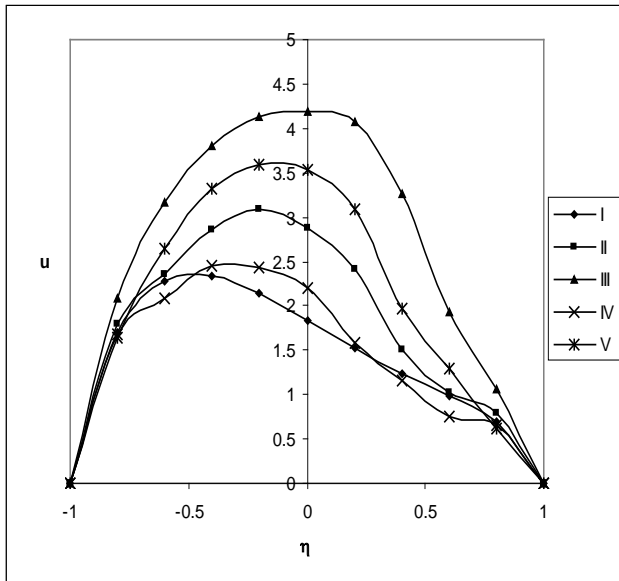


Fig.7: u with M & m

$G=10^3$, $Sc=1.3$, $\alpha=2$, $\beta=0.5$, $k=0.5$

	I	II	III	IV	V
M	2	5	10	2	2
m	0.5	0.5	0.5	1.5	2.5

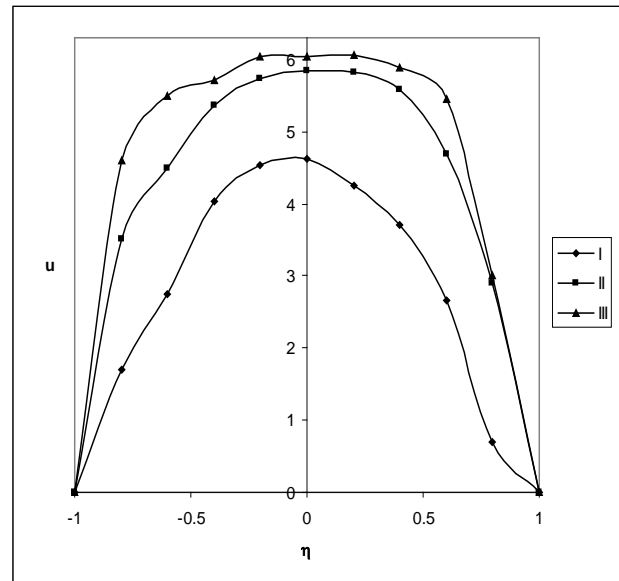


Fig.8: u with α

$M=2$, $m=0.5$, $Sc=1.3$, $\alpha=2$, $\beta=0.5$, $k=0.5$

	I	II	III
α	2	4	6

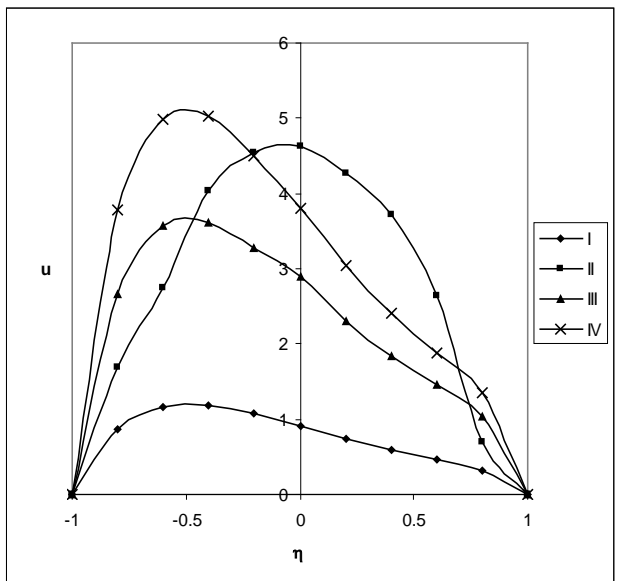


Fig.9: u with β

$G=10^3$, $Sc=1.3$, $\alpha=2$, $\beta=0.5$, $k=0.5$

	I	II	III	IV
β	0.3	0.5	0.7	0.9

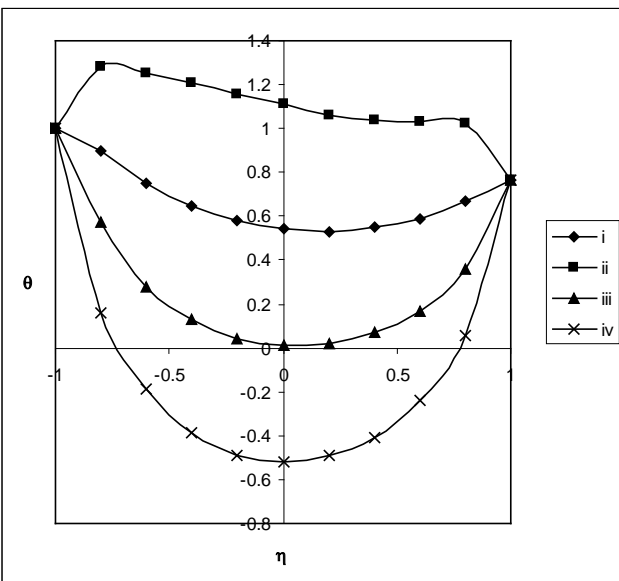


Fig.10: Variation of axial Temperature (θ) with G

$M=2$, $m=0.5$, $Sc=1.3$, $\alpha=2$, $\beta=0.5$, $k=0.5$

	I	II	III	IV
G	10^3	3×10^3	-10^3	-3×10^3

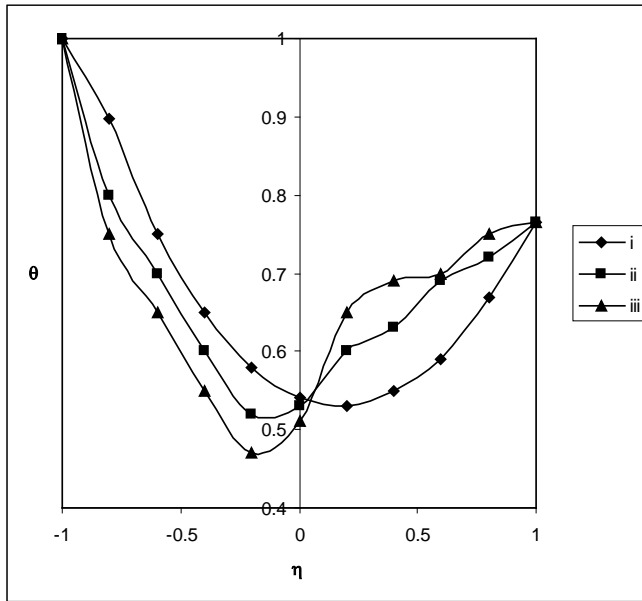


Fig.11: θ with M

$M=2, m=0.5, Sc=1.3, \alpha=2, \beta=0.5, k=0.5$

	I	II	III
M	2	5	10

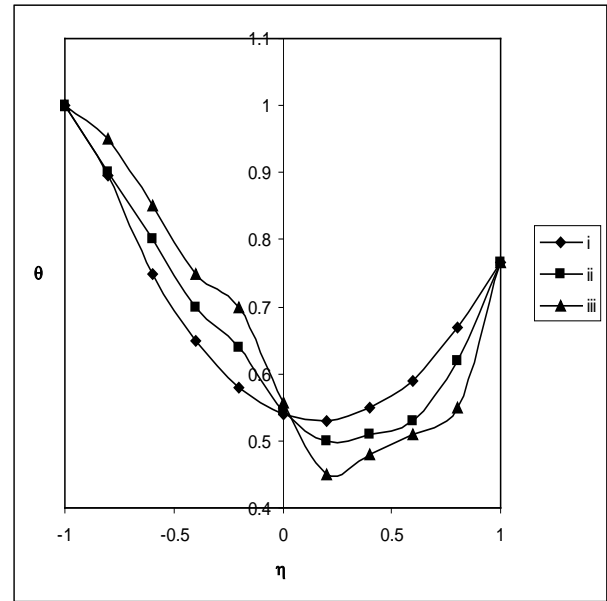


Fig.12: θ with m

$G=10^3, Sc=1.3, \alpha=2, \beta=0.5, k=0.5$

	I	II	III
m	0.5	1.5	2.5

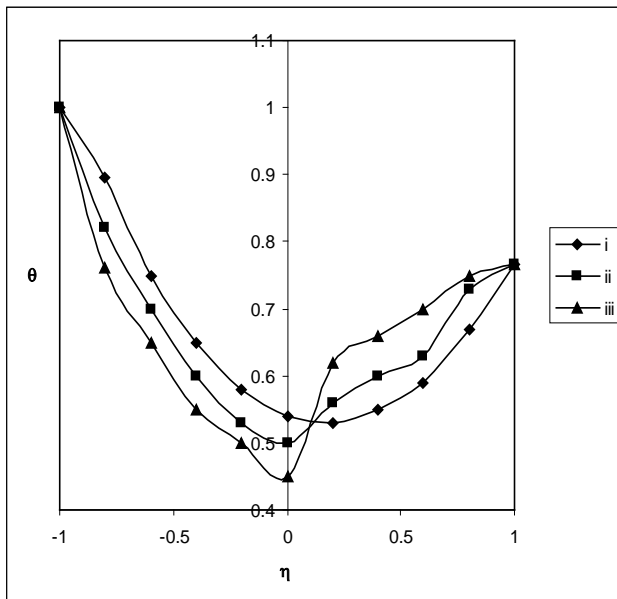


Fig.13: θ with k

$M=2, m=0.5, Sc=1.3, \alpha=2, \beta=0.5, k=0.5$

	I	II	III
k	0.5	1.5	2.5

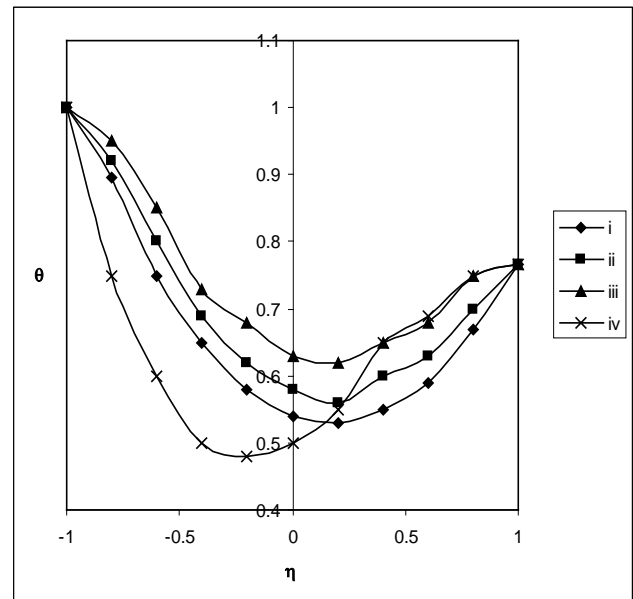


Fig.14: θ with α

$G=10^3, Sc=1.3, \alpha=2, \beta=0.5, k=0.5$

	I	II	III	IV
α	2	4	6	-0.8

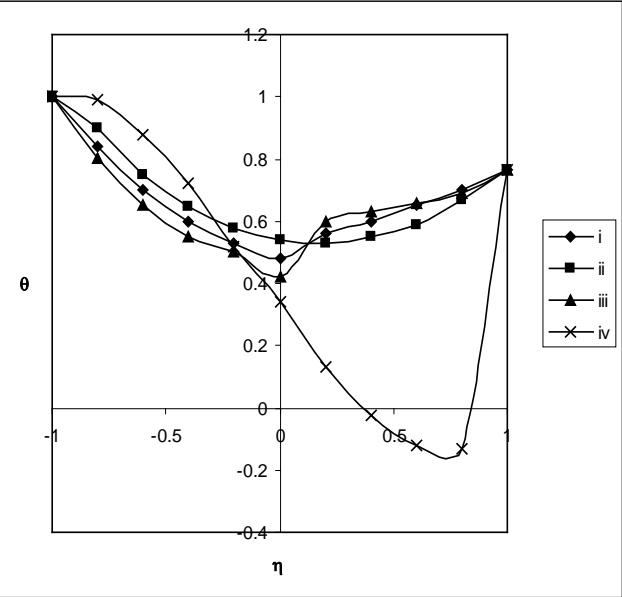


Fig.15: θ with β
 $M=2, m=0.5, Sc=1.3, \alpha=2, \beta = 0.5, k=0.5$
I II III IV
 β 0.3 0.5 0.7 0.9

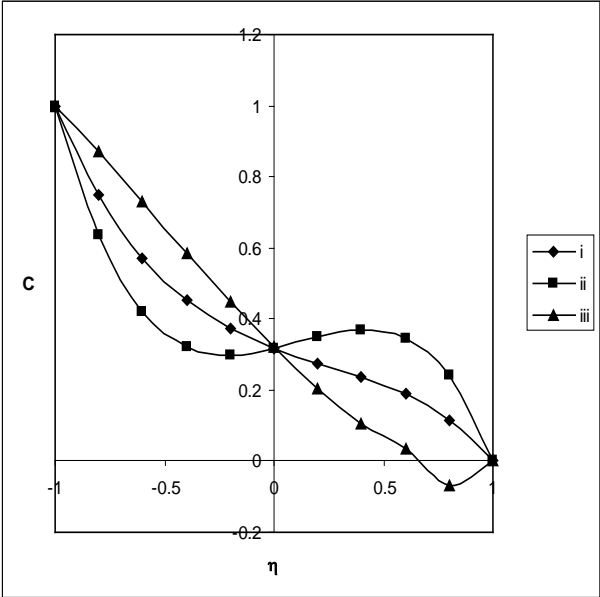


Fig.16: Variation of axial concentration (C) with G
 $M=2, m=0.5, Sc=1.3, \alpha=2, \beta = 0.5, k=0.5, R=35$
I II III
G 10^3 2×10^3 3×10^3

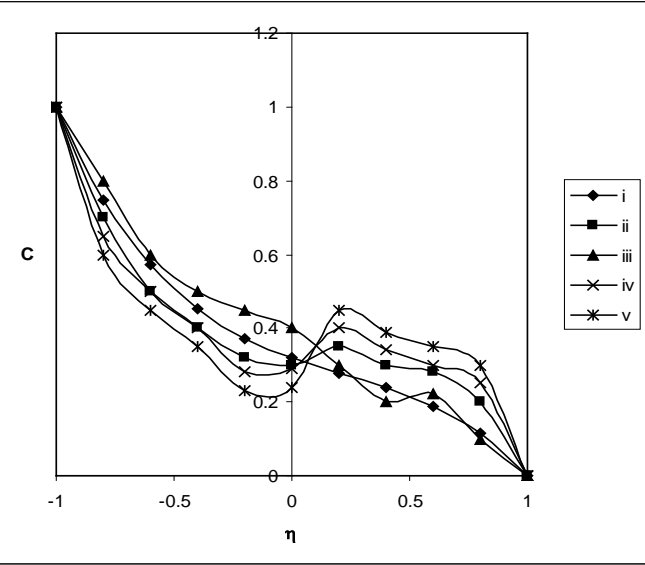


Fig.17: C with R & m
 $G= 10^3, Sc=1.3, \alpha=2, \beta = 0.5, k=0.5$
I II III IV V
R 35 70 140 35 35
m 0.5 0.5 0.5 1.5 2.5

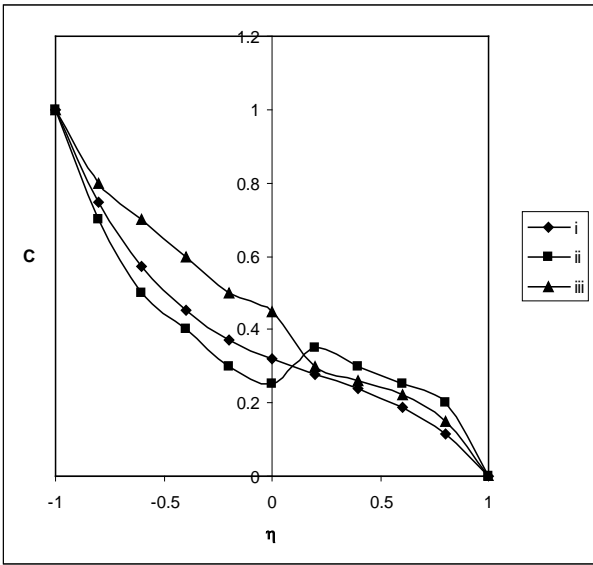


Fig. 18: C with M
 $G= 10^3, m=0.5, Sc=1.3, \alpha=2, \beta = 0.5, k=0.5, R=35$
I II III
M 2 5 10

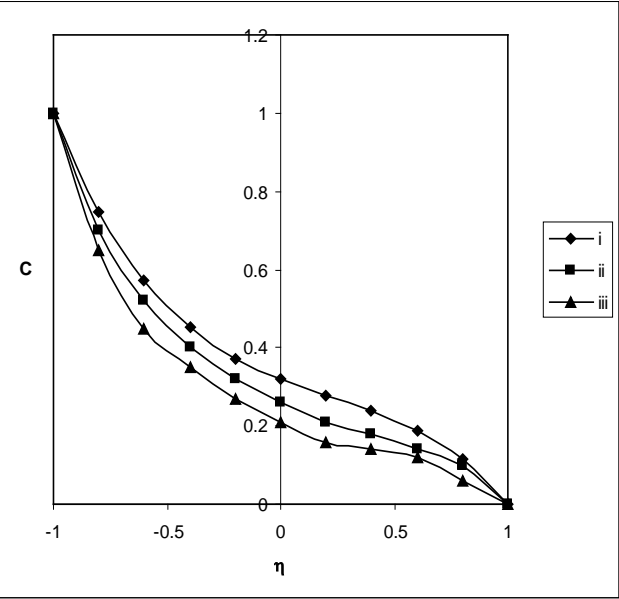


Fig.19: C with k
G= 10³, Sc=1.3, α=2, β = 0.5, k=0.5
I II III
k 0.5 1.5 2.5

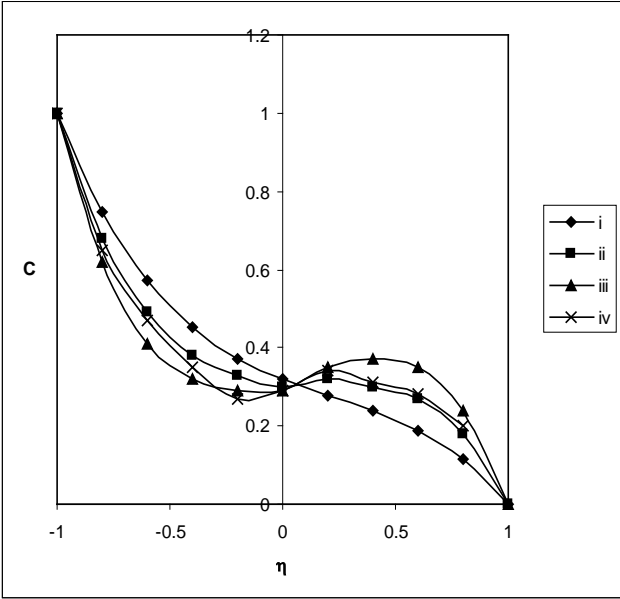


Fig.20: C with α
M=2, m=0.5, Sc=1.3, α=2, β = 0.5, k=0.5, R=35
I II III IV
α 2 4 6 -0.8

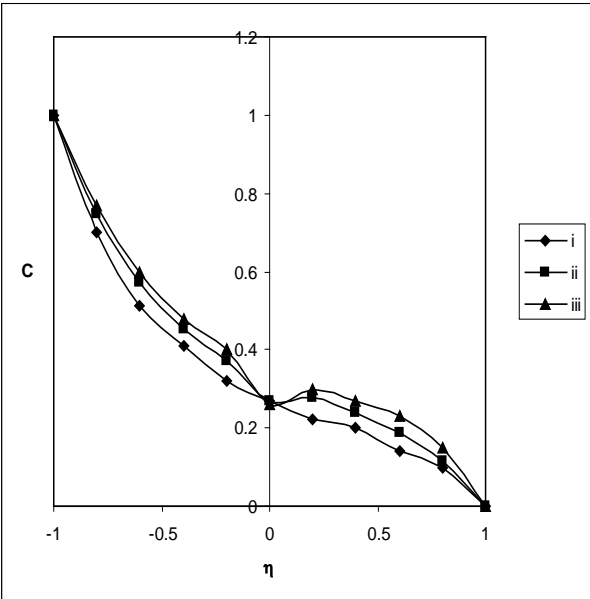


Fig.21: C with β
M=2, m=0.5, Sc=1.3, α=2, β = 0.5, k=0.5, R=35
I II III
β 0.3 0.5 0.7

Table.1
Nu at η=1

G/Nu	I	II	III	IV	V	VI	VII	VIII	IX
10 ³	0.2192	0.5058	0.2123	0.2846	-1.2343	0.1948	0.1833	0.6902	0.6613
3x10 ³	1.0275	1.1842	0.9057	1.4719	1.4921	1.0226	1.0201	1.4652	1.3799
-10 ³	2.4351	2.5129	2.2647	3.8145	4.8666	2.4416	2.4451	2.7707	2.8066
-3x10 ³	1.7416	1.8869	1.6274	2.6388	3.1701	1.7427	1.7433	2.1518	2.1864
K	0.5	1.5	2.5	.5	.5	.5	.5	.5	0.5
α	2	2	2	4	6	2	2	2	2
R	35	35	35	35	35	70	140	35	35
β	0.5	0.5	0.5	0.5	0.5	0.5	0.5	0.3	0.7

Table.2
Nu at $\eta=-1$

G/Nu	I	II	III	IV	V	VI	VII	VIII	IX
10^3	2.4666	2.5323	2.2616	3.0076	3.2264	2.2422	2.1767	2.6909	2.9577
3×10^3	2.2825	2.2923	1.9722	2.9264	3.1772	2.1171	1.9598	2.4517	2.7757
-10^3	1.8793	2.0674	1.7203	2.7013	3.0019	1.8578	1.1809	1.9519	2.5463
-3×10^3	2.0845	2.1945	1.9155	2.8171	3.0968	2.0439	1.5812	2.2076	2.6926
K	0.5	1.5	2.5	.5	.5	.5	.5	.5	0.5
α	2	2	2	4	6	2	2	2	2
R	35	35	35	35	35	70	140	35	35
β	0.5	0.5	0.5	0.5	0.5	0.5	0.5	0.3	0.7

Table.3
Sh at $\eta=1$

G/Nu	I	II	III	IV	V	VI	VII	VII	VIII
10^3	-47.0606	-2.9588	-52.9188	1.9103	3.4594	1.0077	4.8078	5.6377	-6.2429
3×10^3	-2.6361	-1.1695	-2.8695	-1.1042	1.2612	-1.8293	1.7833	-1.8714	-3.0899
-10^3	-0.3688	-.2951	-2.4151	-0.2961	0.0973	-0.1123	0.0724	-0.2592	-0.5181
-3×10^3	2.5767	-1.1795	3.4624	4.5624	7.6119	3.2274	3.9146	1.4888	4.5067
K	0.5	1.5	2.5	.5	.5	.5	.5	.5	0.5
α	2	2	2	4	6	2	2	2	2
R	35	35	35	35	35	70	140	35	35
β	0.5	0.5	0.5	0.5	0.5	0.5	0.5	0.3	0.7

Table.4
Sh at $\eta=-1$

G/Nu	I	II	III	IV	V	VI	VII	VII	VIII
10^3	16.5867	1.1007	2.9988	11.8474	20.6407	21.8051	10.1993	10.0625	-1.9378
3×10^3	-2.0187	-0.5031	2.1831	-1.4296	15.9831	-34.3717	10.8651	-1.1058	-2.7752
-10^3	3.7976	-1.3504	5.0405	6.3924	13.7712	4.6014	5.2474	1.9355	8.3006
-3×10^3	2.5767	-1.1795	3.4624	4.5624	7.6119	3.2274	3.9146	1.4888	4.5067
K	0.5	1.5	2.5	.5	.5	.5	.5	.5	0.5
α	2	2	2	4	6	2	2	2	2
R	35	35	35	35	35	70	140	35	35

Source of support: Nil, Conflict of interest: None Declared